

Ligand-Receptor Interaction Modulates the Energy Landscape of Enzyme-Instructed Self-Assembly of Small Molecules

Richard Haburcak¹, Junfeng Shi¹, Xuewen Du, Dan Yuan, and Bing Xu*

Content

Materials and methods

Peptide synthesis and characterization

Figure S1. Molecular structures of peptides used

Figure S2. Optical image of a hydrogel of **1**

Figure S3. Time-dependent frequency sweep of a solution of **1P**, **2** and ALP

Figure S4. Time-dependent strain sweep of a solution of **1P**, **2** and ALP

Figure S5. TEM and optical images of solutions of **1**, **3** and **4** with various amounts of **2**

Figure S6. ITC of **1P** into **2** in PBS with or without ALP

Figure S7. ITC of **2** into PBS buffer

Figure S8. ITC of **2** into solutions of **3**, **3P**, **4**, **4P** in PBS

Figure S9. ITC of **1P** into PBS with varying amounts of **2** and ALP

Figure S10. ITC of **2** into solution of **3** in PBS with 1% and 4% Tween-80

Figure S11. ITC of **2** into solution of **4** in PBS with 1% and 4% Tween-80

Figure S12. ITC of **2** into PBS with 1% and 4% Tween-80

Figure S13. Hydrodynamic radius from DLS of various concentrations of Tween-80 in PBS

Figure S14. Light scattering signal of **1** and **2** in PBS with various concentrations of Tween-80

Figure S15. TEM micrographs of solutions of 0.8mM **1** with various concentrations of Tween-80

Figure S16. TEM micrographs of solutions of **3**, **3P**, **2** and ALP

Figure S17. TEM micrographs of solutions of **4**, **4P**, **2** and ALP

Figure S18. TEM micrographs of solutions of **3&2** and **4&2** in the presence of various concentrations of Tween-80

Figure S19. Time-dependent TEM of a solution of **1P**, **2**, and various concentrations of ALP

Figure S20. TEM of a solution of **1P**, ALP and vancomycin aglycon

Figure S21. TEM of solution of **1** with hexafluoroisopropanol

Materials and Methods

Materials. Vancomycin, N,N-diisopropylethylamine (DIPEA), piperidine, and O-benzotriazole-N,N,N',N'-tetramethyl-uronium-hexafluoro-phosphate (HBTU) were purchased from ACROS Organics USA; all amino acid derivatives from GL Biochem (Shanghai) Ltd.

Instrumentation. LC-MS on Waters Acuity Ultra Performance LC with Waters MICROMASS detector; isothermal titration calorimetry on Nano ITC (TA); TEM on Morgagni 268 transmission electron microscope; rheology on TA ARES-G2 rheometer.

Peptide synthesis and purification. All compounds were prepared by solid-phase peptide synthesis (SPPS) using 2-chlorotrityl chloride resin.² The first amino acid was loaded onto the resin at the C-terminal, followed by removal of the Fmoc protecting group by treatment with 20% piperidine. The next Fmoc-protected amino acid was coupled to the free amino group using N,N-Diisopropylethylamine/O-Benzotriazole-N,N,N',N'-tetramethyl-uronium-hexafluoro-phosphate(DIPEA/HBTU) as the coupling reagent. Further deprotection and coupling steps followed established Fmoc- SPPS protocols. As the final step, the resin-bound peptide was cleaved using a cocktail of TFA/triisopropylsilane/water (95: 2.5: 2.5) for 2h under a nitrogen atmosphere, the cleavage solution was collected. The resin was further washed twice with TFA, and the filtrate was collected. Crude product was obtained after the addition of cold diethyl ether into concentrated filtrate. The crude product was purified by reverse phase high performance liquid chromatography (HPLC) using a semi-prepare C18 column. HPLC solvents consisted of solvent A (0.1% TFA in water) and solvent B (0.1% TFA in acetonitrile). The resulting peptide solution was frozen and lyophilized to afford purified compounds in around 80% yields after purification.

1P: ¹H NMR (400 MHz, DMSO-*d*₆) δ 12.48 (bs, 1H), 9.15 (s, 1H), 8.25 (d, *J* = 8.6 Hz, 1H), 8.16 (d, 1H), 8.13 (d, *J* = 7.3 Hz, 2H), 8.04 – 7.91 (m, 2H), 7.87 – 7.82 (m, 1H), 7.80 – 7.75 (m, 1H), 7.73 (d, *J* = 8.5 Hz, 2H), 7.57 (bs, 1H), 7.46 (m, 1H), 7.26 – 7.07 (m, 7H), 7.03 (d, *J* = 8.5 Hz, 1H), 6.64 (d, *J* = 8.4 Hz, 1H), 4.60 – 4.39 (m, 2H), 4.33 (ddd, 1H), 4.17 (ddd, *J* = 7.3 Hz, 1H), 3.80 – 3.66 (m, 3H), 3.56 (d, *J* = 14.1 Hz, 1H), 3.47 (d, *J* = 14.1 Hz, 1H), 3.05 – 2.85 (m, 2H), 2.83 – 2.62 (m, 2H), 1.26 (d, *J* = 7.3 Hz, 2H), 1.20 (d, *J* = 7.1 Hz, 2H). ³¹P NMR (81 MHz, DMSO-*d*₆) δ -6.24 (s).

1: ¹H NMR (400 MHz, DMSO-*d*₆) δ 9.22 (s, 1H), 8.26 (d, *J* = 8.4 Hz, 1H), 8.21 – 8.09 (m, 4H), 7.98 (d, *J* = 6.6 Hz, 2H), 7.84 (d, *J* = 7.5 Hz, 1H), 7.76 (d, *J* = 7.3 Hz, 1H), 7.72 (d, *J* = 8.5 Hz, 1H), 7.56 (s, 1H), 7.52 – 7.40 (m, 2H), 7.22 – 7.09 (m, 12H), 7.03 (d, *J* = 8.3 Hz, 2H), 6.64 (d, *J* = 8.4 Hz, 2H), 4.55 – 4.40 (m, 3H), 4.37 – 4.26 (m, 1H), 4.22 – 4.08 (m, 1H), 3.72 (d, *J* = 5.0 Hz, 4H), 3.55 (d, *J* = 13.9 Hz, 2H), 3.02 – 2.87 (m, 3H), 2.73 (dd, *J* = 17.9, 8.1 Hz, 3H), 1.25 (d, *J* = 7.3 Hz, 3H), 1.20 (d, *J* = 7.1 Hz, 3H).

3P: ^1H NMR (400 MHz, DMSO- d_6) δ 8.31 – 8.22 (m, 3H), 8.22 – 8.14 (m, 2H), 8.08 (t, J = 5.7 Hz, 1H), 8.02 (d, J = 7.7 Hz, 1H), 7.85 (d, J = 7.4 Hz, 1H), 7.77 (d, J = 7.5 Hz, 1H), 7.73 (d, J = 8.5 Hz, 1H), 7.57 (s, 1H), 7.51 – 7.40 (m, 2H), 7.27 – 7.11 (m, 13H), 7.06 (d, J = 8.3 Hz, 2H), 4.61 – 4.44 (m, 3H), 4.38 – 4.26 (m, 1H), 4.21 – 4.09 (m, 2H), 3.82 – 3.69 (m, 4H), 3.51 (dd, J = 39.8, 13.9 Hz, 3H), 3.07 – 2.88 (m, 3H), 2.87 – 2.75 (m, 2H), 2.75 – 2.62 (m, 2H), 1.26 (d, J = 7.3 Hz, 3H), 1.20 (d, J = 7.0 Hz, 3H). ^{31}P NMR (81 MHz, DMSO- d_6) δ -6.25 (s).

3: ^1H NMR (400 MHz, DMSO- d_6) δ 9.18 (s, 1H), 8.28 (d, J = 8.7 Hz, 1H), 8.23 – 8.13 (m, 4H), 8.02 (d, J = 6.7 Hz, 2H), 7.85 (d, J = 7.3 Hz, 1H), 7.77 (d, J = 7.2 Hz, 1H), 7.73 (d, J = 8.5 Hz, 1H), 7.57 (s, 1H), 7.46 (p, J = 6.6 Hz, 2H), 7.24 – 7.08 (m, 10H), 7.03 (d, J = 8.4 Hz, 2H), 6.64 (d, J = 8.4 Hz, 2H), 4.59 – 4.43 (m, 3H), 4.39 – 4.28 (m, 2H), 4.21 – 4.11 (m, 2H), 3.76 – 3.70 (m, 4H), 3.51 (dd, J = 38.4, 14.0 Hz, 2H), 3.05 – 2.86 (m, 3H), 2.82 – 2.63 (m, 3H), 1.26 (d, J = 7.3 Hz, 3H), 1.20 (d, J = 7.0 Hz, 3H).

4P: ^1H NMR (400 MHz, DMSO- d_6) δ 8.36 (d, J = 7.9 Hz, 1H), 8.28 – 8.19 (m, 3H), 8.18 (d, J = 7.1 Hz, 1H), 8.09 – 7.98 (m, 2H), 7.84 (d, J = 8.1 Hz, 1H), 7.77 (d, J = 8.0 Hz, 1H), 7.73 (d, J = 8.7 Hz, 1H), 7.57 (s, 1H), 7.51 – 7.40 (m, 2H), 7.25 – 7.09 (m, 17H), 7.05 (d, J = 7.9 Hz, 3H), 4.60 – 4.43 (m, 3H), 4.37 – 4.29 (m, 1H), 4.23 – 4.12 (m, 1H), 3.74 (d, J = 5.1 Hz, 4H), 3.51 (dd, J = 41.8, 14.0 Hz, 5H), 3.06 – 2.86 (m, 4H), 2.86 – 2.63 (m, 4H), 1.25 (d, J = 7.3 Hz, 3H), 1.20 (d, J = 7.1 Hz, 3H). ^{31}P NMR (81 MHz, DMSO- d_6) δ -5.7 (s).

4: ^1H NMR (400 MHz, DMSO- d_6) δ 9.21 (bs, 1H), 8.33 (s, 1H), 8.22 (bs, 3H), 8.15 (d, J = 6.1 Hz, 1H), 8.05 (d, J = 7.4 Hz, 1H), 8.00 (s, 1H), 7.84 (d, J = 8.0 Hz, 1H), 7.77 (d, J = 7.7 Hz, 1H), 7.73 (d, J = 8.5 Hz, 1H), 7.57 (s, 1H), 7.52 – 7.38 (m, 2H), 7.25 – 7.09 (m, 12H), 7.03 (d, J = 8.0 Hz, 2H), 6.64 (d, J = 7.9 Hz, 2H), 4.58 – 4.42 (m, 3H), 4.38 – 4.25 (m, 1H), 4.23 – 4.06 (m, 1H), 3.72 (s, 3H), 3.51 (dd, J = 39.6, 14.1 Hz, 2H), 3.01 – 2.84 (m, 3H), 2.80 – 2.63 (m, 3H), 1.26 (d, J = 7.3 Hz, 3H), 1.20 (d, J = 7.0 Hz, 3H).

TEM measurement. Aliquots (3-5 μL) of sample solutions were added into glow discharge thin carbon-coated copper grids (400 meshes, Pacific Grid-Tech) and incubated for 30s at room temperature. Excess sample solution was removed by blotting with filter paper touched to the edge of the grid. After removing excess fluid, the grid was washed with three successive drops of deionized water and then exposed to three successive drops of 2.0% (w/v) uranyl acetate. Data were collected at high vacuum on Morgagni 268 transmission electron microscope.

Rheological measurement. Rheological tests were conducted on TA ARES-G2 rheometer, parallel-plate geometry with an upper plate diameter of 25 mm was used during the experiment, and the gap was 0.4 mm. During the measurement, the stage temperature was maintained at 25 $^\circ\text{C}$ by a peltier heating cooling system. The samples were loaded into the stage, and the upper plate was slowly lowered onto the sample. After 10-30 minutes in the experimental configuration, the rheological tests were performed: strain sweep (0.1-100%) at 6.28 rad/s, frequency sweep test (0.1-200 rad/s).

Isothermal titration calorimetry. The compounds were dissolved in pH 7.4 PBS buffer at suitable concentrations. Titration experiments were performed on a Nano ITC (Isothermal titration calorimetry, 170 μL) with a gold reaction vessel. The reference cell was filled with 400 μL DI water. Typically, each titration experiment consisted of 25 x 2 μL injections at 600 s intervals with a stirring speed of 250 rpm. A 300 s or 600 s baseline was collected before the next injection. The experiments were conducted at 25 $^\circ\text{C}$.

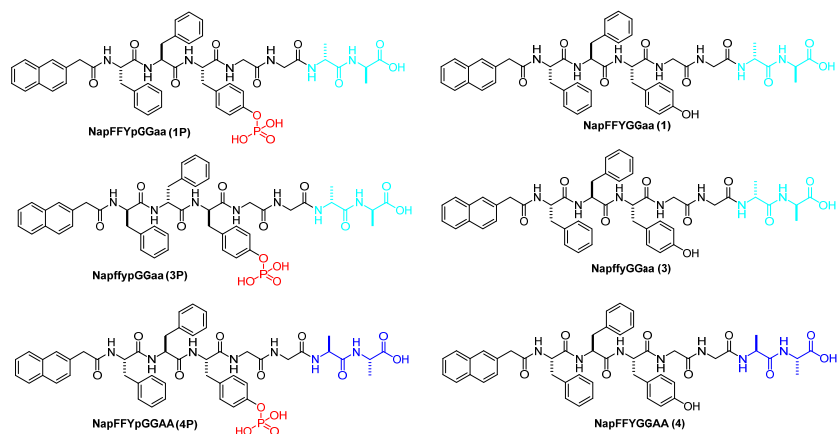


Figure S1. Molecular structures of synthesized receptor derivatives.



Figure S2. Optical image of a gel of **1** at 4 mM, pH 6.4.

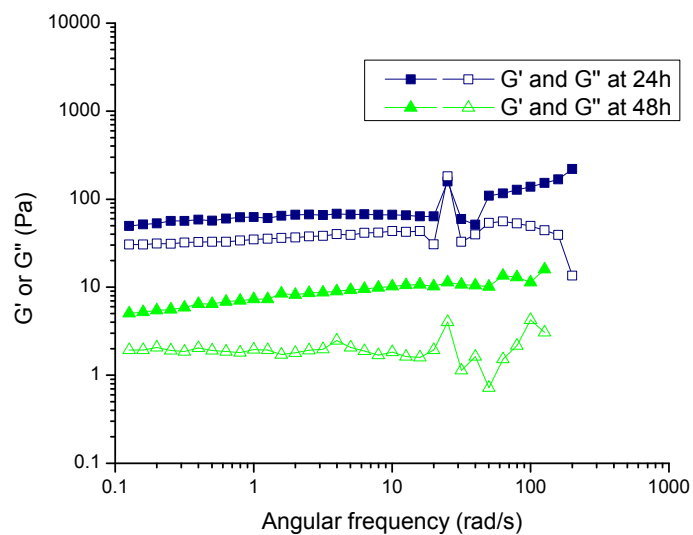


Figure S3. Frequency sweep showing storage and loss moduli of the suspension of **1P**, **2**, and ALP at 24 and 48 hours. $[1P]_0 = [2] = 500 \mu\text{M}$, $[ALP] = 1.25 \text{ U/mL}$.

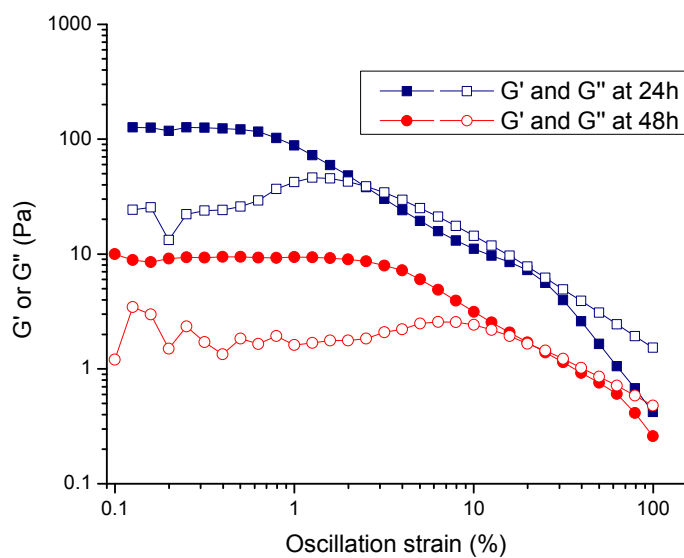


Figure S4. Strain sweep showing storage and loss moduli of the suspension of **1P**, **2** (Van), and ALP at 24 and 48 hours. $[1P]_0 = [2] = 500 \mu\text{M}$, $[ALP] = 1.25 \text{ U/mL}$.

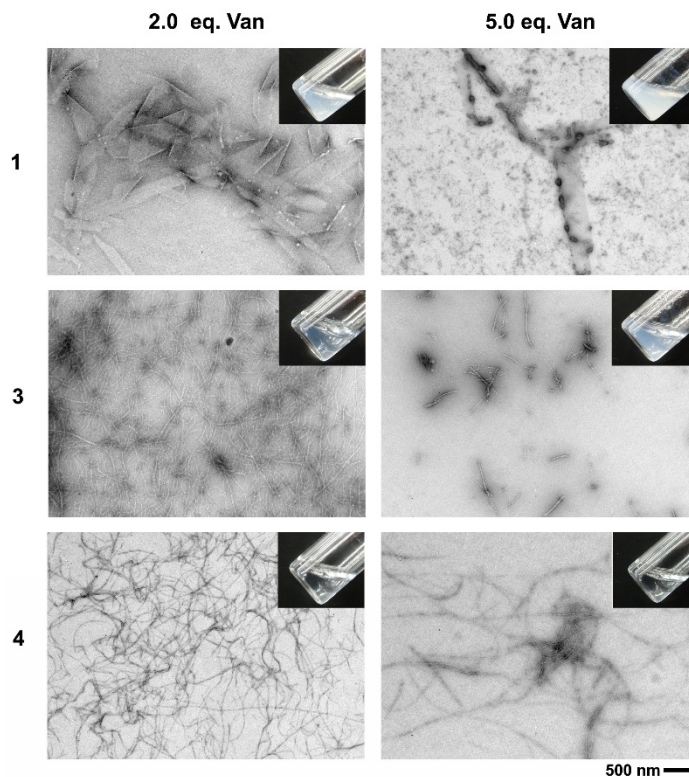


Figure S5. TEM images and optical images of solution of **1**, **3**, and **4** 24-48 hours after addition of different amounts of Van. $[1] = [3] = [4] = 500 \mu\text{M}$.

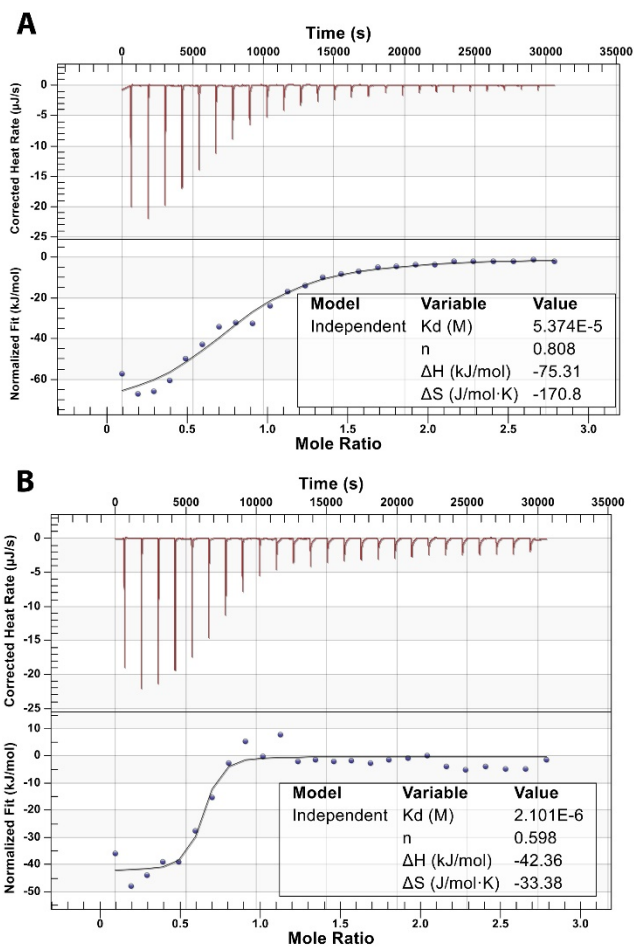


Figure S6. Isothermal titration of **1P** (4.0 mM) into Van (0.5 mM) without (A) or with (B) ALP (1.67 U/mL).

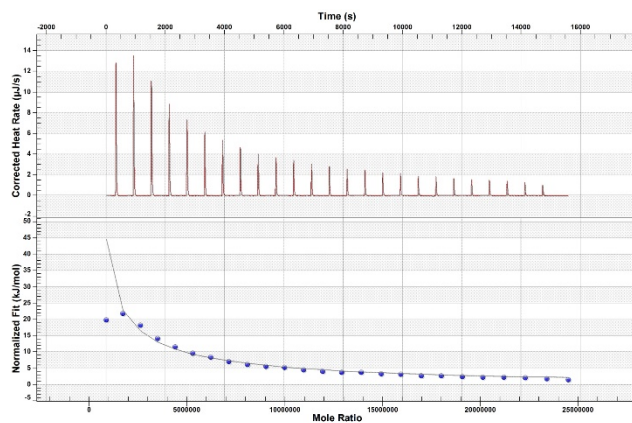


Figure S7. Isothermal titration of Van (8.0 mM) into PBS buffer.

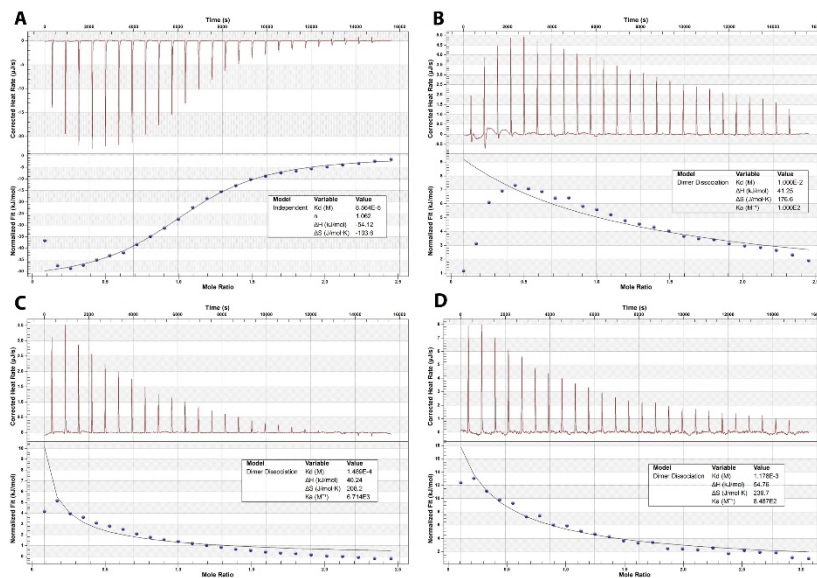


Figure S8. Isothermal titrations of A) **3P**, B) **3**, C) **4P**, and D) **4** with Van at 25 °C for the determination of dissociation constant (K_d) and stoichiometry (n).

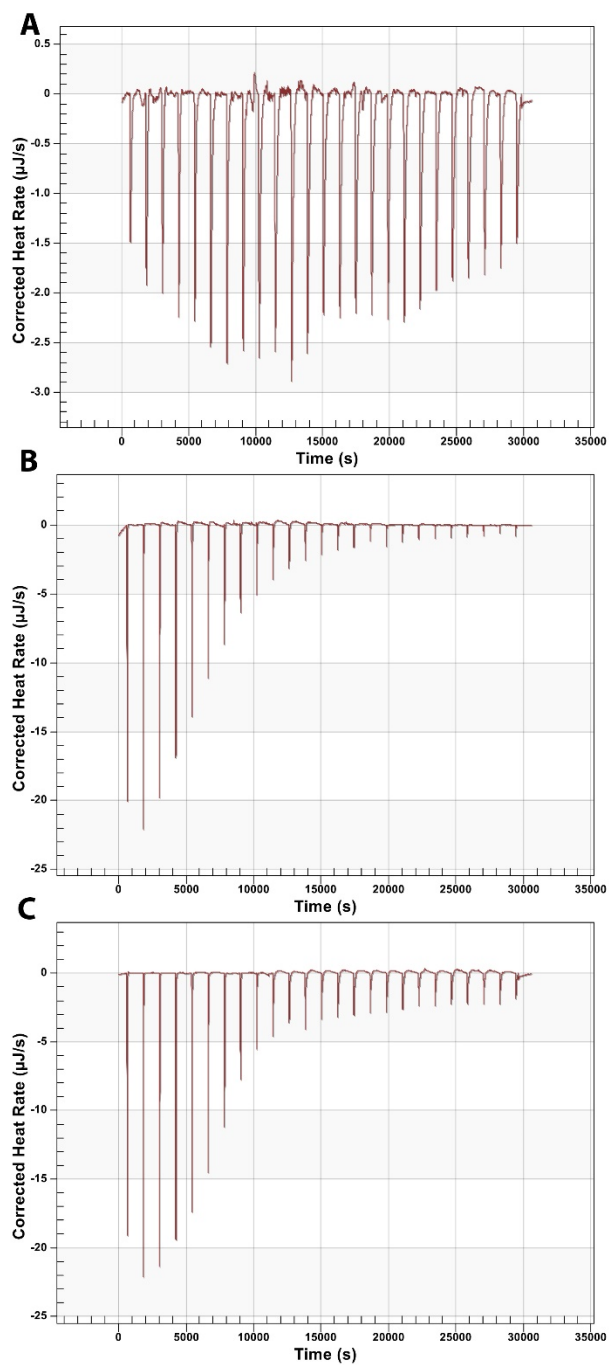


Figure S9. Isothermal titrations of **1P** (4 mM) into PBS buffer at pH7.4 with (a) 1.67 U/mL ALP, (b) 0.5 mM Van, (c) 1.67 U/mL ALP and 0.8 mM Van.

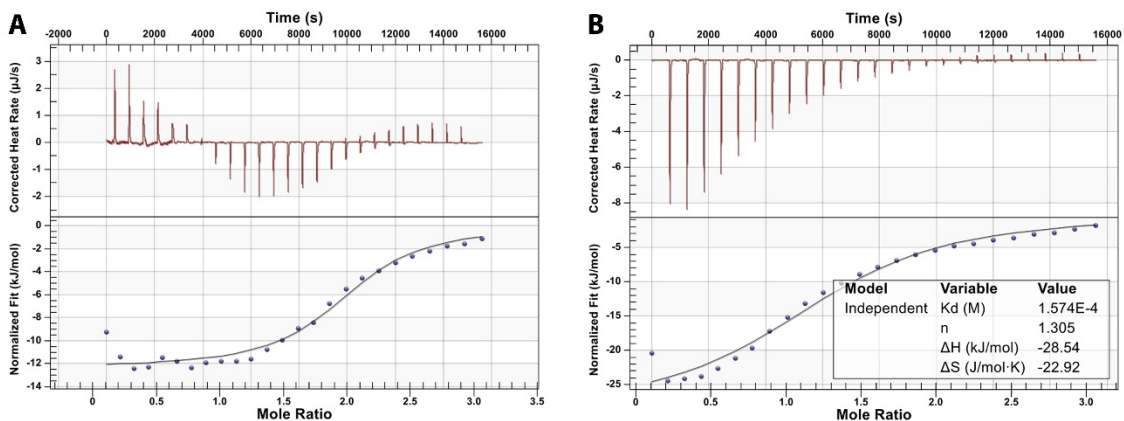


Figure S10. Isothermal titrations of **3** with Van in the presence of 1.0 % (a) and 4.0 % (b) Tween-80.

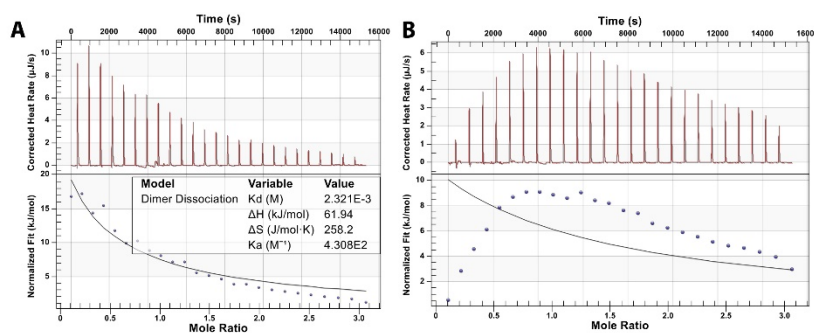


Figure S11. Isothermal titrations of **4** with Van in the presence of 1.0 % (a) and 4.0 % (b) Tween-80.

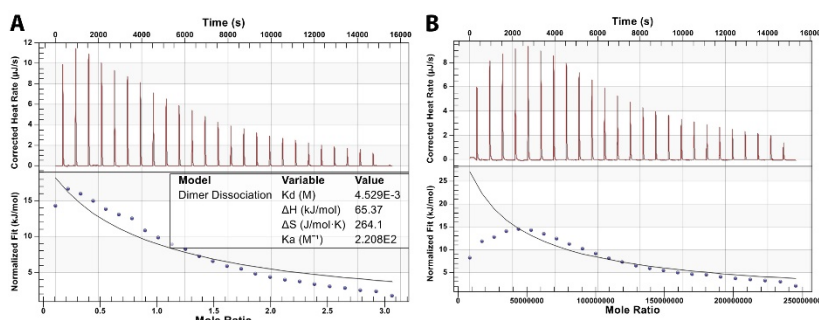


Figure S12. Isothermal titrations of Van (8 mM) into PBS buffer in the presence of 1.0 % (a) and 4.0 % (b) Tween-80.

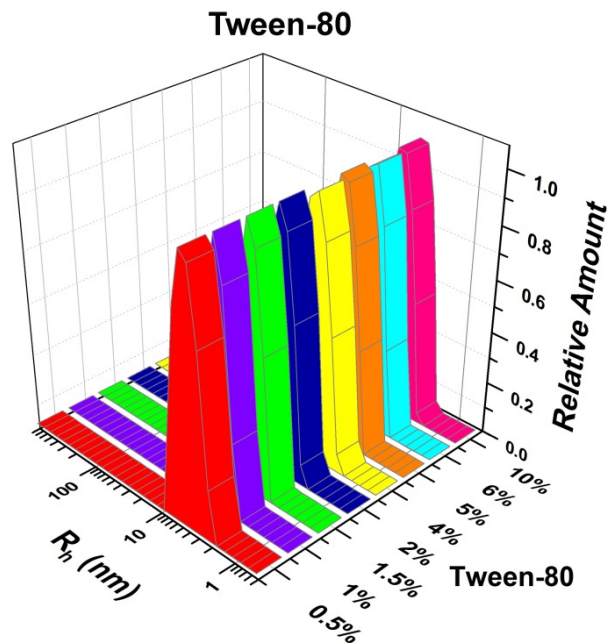


Figure S13. Hydrodynamic radius (R_h) of Tween-80 at various concentrations.

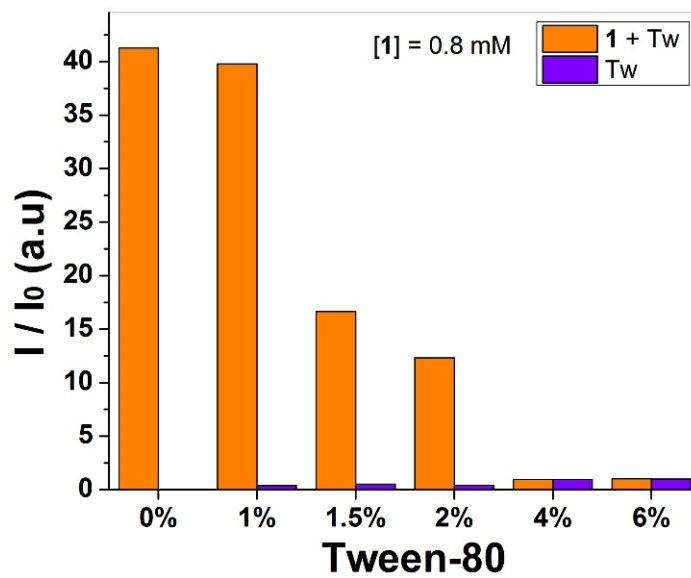


Figure S14. Light scattering signal (I/I_0) for the solution of Tw-80 and 1& Tw-80 at different concentrations.

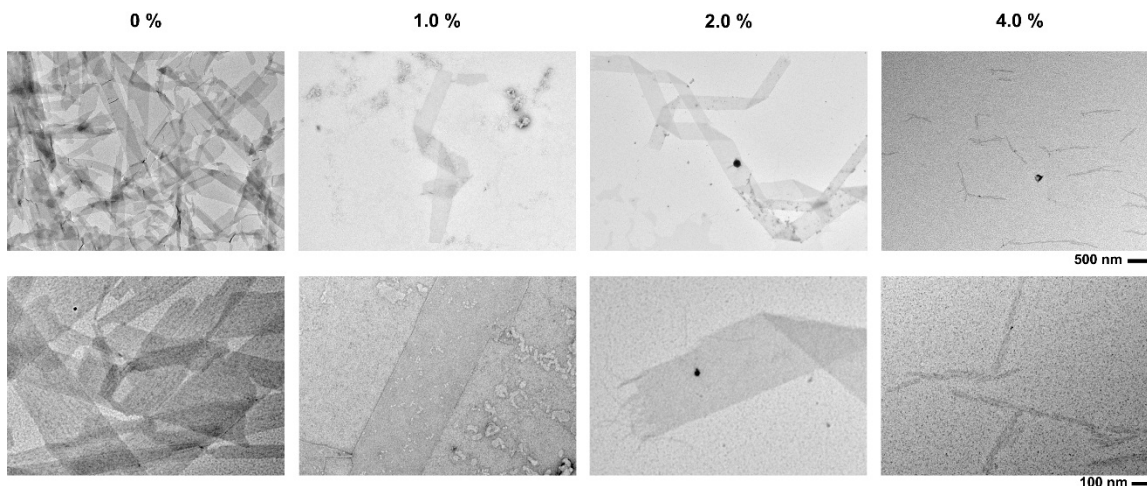


Figure S15. TEM images of solution of **1** (0.8 mM) in the presence of various amount of Tween-80.

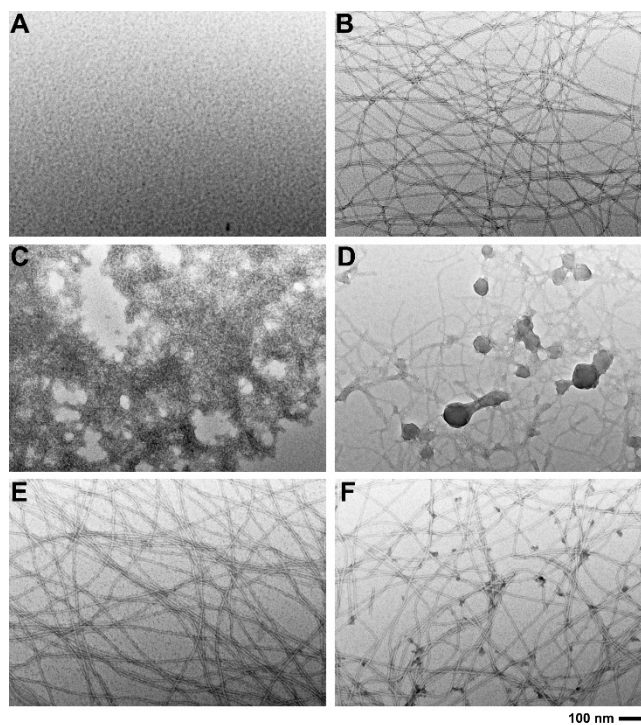


Figure S16. TEM images of (A) solution of **3P**, (B) **3P**+ALP, (C) suspension of **3P**&Van, (D) **3P**&Van+ALP, (E) **3**, and (F) **3**&Van. $[3P]_0 = [3]_0 = [Van]_0 = 500 \mu\text{M}$, ALP = 1.25 U/mL.

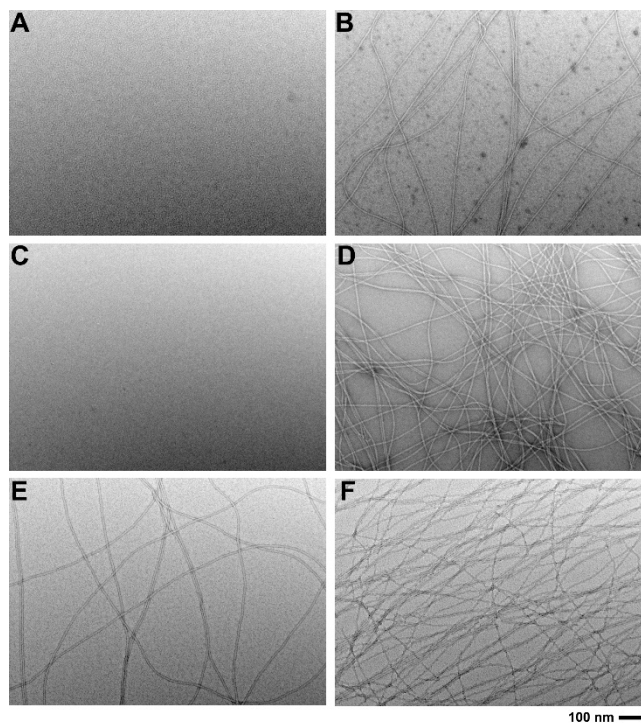


Figure S17. TEM images of (A) solution of **4P**, (B) **4P**+ALP, (C) suspension of **4P**&Van, (D) **4P**&Van+ALP, (E) **4**, and (F) **4**&Van. $[4P]_0 = [4]_0 = [Van]_0 = 500 \mu\text{M}$, ALP = 1.25 U/mL.

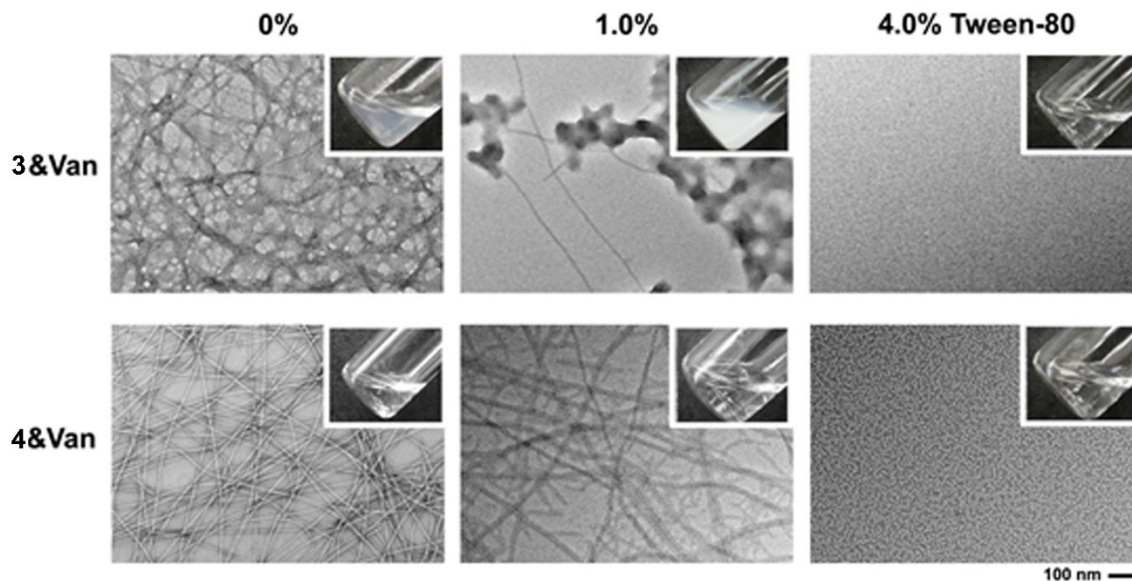


Figure S18. TEM images and optical images (inset) of solution of **3**&Van and **4**&Van upon the addition of various amount of Tween-80.

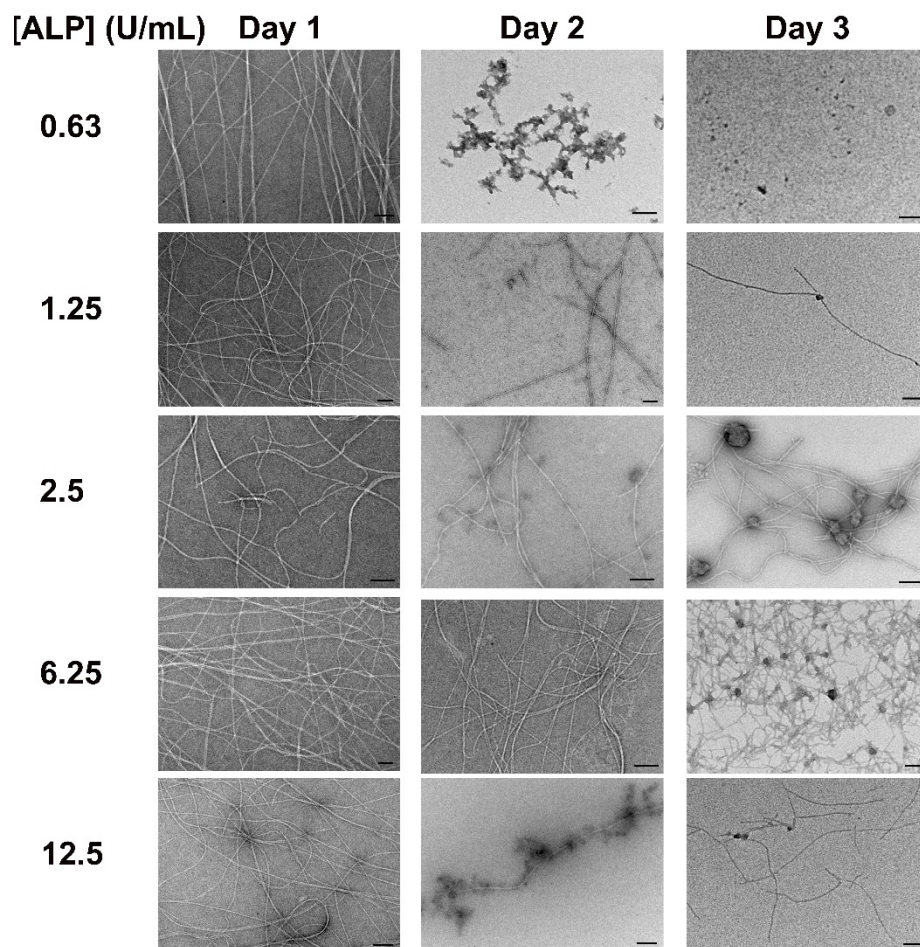


Figure S19. TEM micrographs taken on three consecutive days of suspensions of **1P**, **2**, and ALP, with varying concentrations of ALP. $[\mathbf{1P}]_0 = [\mathbf{2}]_0 = 500 \mu\text{M}$, pH = 7.6, each scale bar is 100 nm.

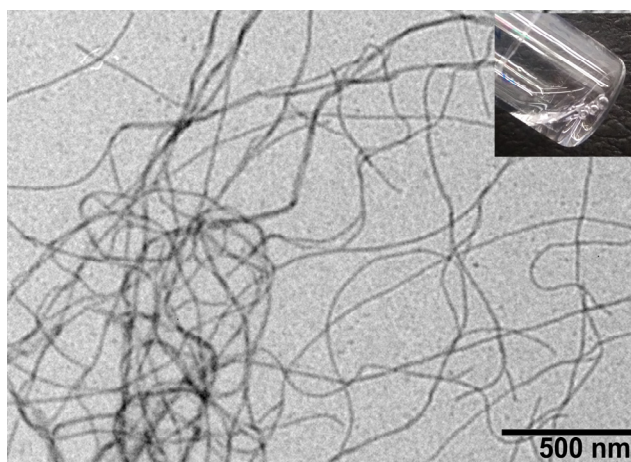


Figure S20. TEM micrograph of a suspension of **1P**, ALP, and glycan-free **2**. Inset is the optical image of the suspension. $[\mathbf{1P}] = [\text{Aglycon } \mathbf{2}] = 500\mu\text{M}$, $[\text{ALP}] = 1.25 \text{ U/mL}$.

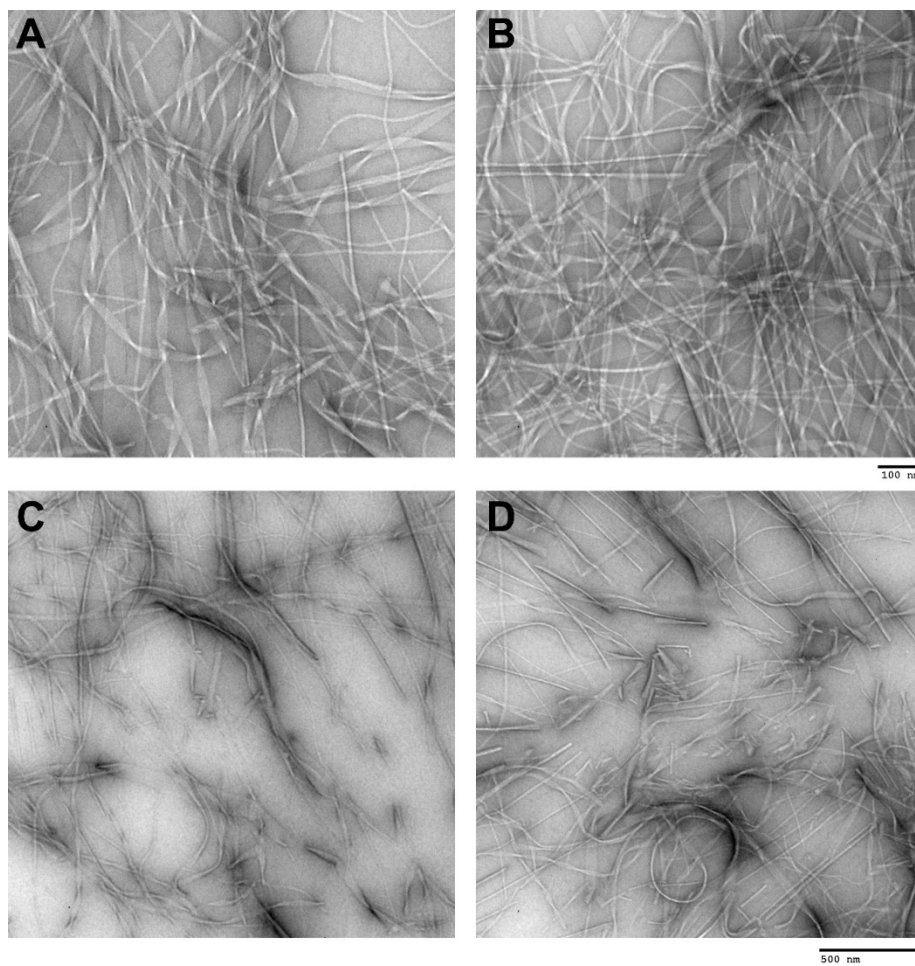


Figure S21. TEM images of a 500 μM solution of **1** at pH 7.4, 7 days after dispersion in PBS buffer. The peptide was first dissolved in hexafluoroisopropanol which was removed under a stream of nitrogen prior to dispersion in buffer. Scale bar is 100 nm for (A) and (B) and 500 nm for (C) and (D).